

The Voltage-Gating Process of the Voltage-Dependent Anion Channel Is Sensitive to Ion Flow

Martin Zizi,* Cynthia Byrd,# Roland Boxus,* and Marco Colombini#

*Department of Physiology, K.U. Leuven Medical School, Campus Gasthuisberg, Leuven 3000, Belgium, and #Department of Biology, University of Maryland, College Park, Maryland 20742 USA

ABSTRACT The voltage-dependent anion channel (VDAC) is a voltage-gated channel from the mitochondrial outer membrane. It has two gating processes: one at positive potentials and the other at negative potentials. The energetics of VDAC gating are quite different when measured in the presence or absence of an ion gradient. A positive potential on the high-salt side results in channel closure at lower transmembrane potentials. The midpoint potential (V_0) shifted from 25 to 5.7 mV, with an activity gradient for KCl of 0.6 versus 0.06. The opposite occurred for negative potentials on the high-salt side (V_0 shifted from -25 to -29 mV). Thus the salt gradient favored closure for one gating process and opening for the other. These results could be explained if part of the electrochemical potential of the gradients present were transferred to the gating mechanism. If the kinetic energy of the ion flow were coupled to the gating process, the effects of the gradient would depend on the mass and velocities of these ions. This was tested by using a series of different salts (KCl, NaCl, LiCl, KBr, K acetate, Na butyrate, and RbBr) under an identical activity gradient. The kinetic energy correlated very well with the measured shifts in free energy of the channel gating. This was true for both polarities. Thus the gating of VDAC is influenced by ion flow. These results are consistent in sign and direction with the voltage gating process in VDAC, which is believed to involve the movement of a positively charged portion of the wall of the channel out of the membrane.

INTRODUCTION

Unlike transistors, voltage-gated channels studied so far are strictly voltage-dependent devices. When a channel protein changes its conformation (open-closed being the simplest case) under a varying electric field, voltage dependence could arise if the structural change resulted in 1) charged domain moving relative to the electric field or 2) a rotation of the dipole moment of the voltage sensor domain relative to the electric vector. These two (nonexclusive) processes would allow mechanical work to be performed on the protein by the electric field. If these processes are coupled to a functional change in the protein (e.g., the opening or closing of the channel), then the protein domains involved form what is referred to as the voltage sensor. Different types of voltage-sensing domains have been proposed and/or reported (e.g., Catterall, 1986; Merrill and Cramer, 1990; Thomas et al., 1993; Colombini, 1994), and they are presumed to be strictly voltage sensitive.

This paradigm may not be totally correct for large channels like porins, GAP junctions, or VDACs. These channels form aqueous pores that are needed to facilitate the flow of large solutes (substrates, nucleotides, etc.) across cell membranes. Thus channel closure involves forming an obstruction against a solution that begins to have bulk properties. Unlike the high-molecular-weight channels that form narrow pores, some of these channels use 10 times less protein

to form a much larger aqueous pore, increasing the likelihood that the mechanical properties of the fluid will influence the structure of the protein. For VDAC, the voltage-sensing domain is also part of the wall of the pore when the channel is in the open state (Peng et al., 1992; Thomas et al., 1993). Thus flow within the channel would be in mechanical contact with the voltage sensor domain.

VDAC has two voltage-gating processes: one observed at positive and the other at negative potentials. Under the conditions generally used to study these channels (reconstitution into membranes made from soybean phospholipids), VDAC behaves symmetrically in that closure is observed at both positive and negative potentials with virtually the same steepness of voltage dependence (parameter n) and the same magnitude of potential (V_0). In the presence of an ion gradient, the gating processes shift. The gradient favors channel closure for one gating process and opening for the other. From a thermodynamical point of view, this can only happen if there is a transfer, or interaction, between the potential energy stored in the ion gradient and the energetics of the gating mechanism. One possible coupling could be the transfer of kinetic energy from the ion gradient to the moving voltage sensor during channel opening and closure. This was tested by using different permeant ions, and therefore different hydrated masses and velocities, under a constant activity gradient. The kinetic energies correlated very well with the energetics of the gating. This effect cannot be explained by differences in ion mobilities only. Likewise, water depletion from the channel lumen by an osmotic effect of impermeant ions as it has been already shown for polymers (Zimmerberg and Parsegian, 1986) cannot account for our results. It is thus concluded that the voltage sensor and therefore the voltage gating of VDAC are sen-

Received for publication 8 September 1997 and in final form 21 April 1998.

Address reprint requests to Dr. Martin Zizi, Department of Physiology, K.U. Leuven Medical School, Campus Gasthuisberg, Leuven 3000, Belgium. Tel.: 32-16-34-5728; Fax: 32-16-34-5991; E-mail: martin.zizi@med.kuleuven.ac.be.

© 1998 by the Biophysical Society

0006-3495/98/08/704/10 \$2.00

sitive to ion flow. Moreover, the reported effect is consistent in sign and direction with the proposed gating mechanism for VDAC, which involves the motion of a rather large portion of the wall of the pore.

MATERIALS AND METHODS

The reconstitution system

Planar phospholipid membranes were formed according to the method of Montal and Mueller (1972), modified as described (Colombini, 1987). The membranes were formed across a 0.10-mm hole in a Saran partition separating two identical teflon hemichambers containing the bathing solutions. The membrane was voltage clamped, and the current across the membrane was recorded. Calomel electrodes were used to interface with the aqueous solutions. After sufficient VDAC channels had inserted into the membrane, the voltage gating was probed by using slow (5.0 mHz) triangular voltage waves. Because the reopening of VDAC is fast (submillisecond range), this allowed current recordings from a channel population in quasithermodynamical equilibrium. Thus the Boltzmann distribution may be used as has been done traditionally (Ehrenstein et al., 1970; Schein et al., 1976):

$$\frac{[\text{closed}]}{[\text{open}]} = \exp \frac{(nFV - nFV_0)}{RT} \quad (1)$$

where V is the transmembrane voltage; V_0 is the voltage at which half the channels are open; n is the net effective gating valence (a measure of the steepness of the voltage dependence); and R , F , and T have their usual meanings. Because VDAC channels are conductive in the "closed" state, the ratio of the concentration of open to closed channels was determined as follows:

$$\frac{[\text{closed}]}{[\text{open}]} = \frac{G_{\max} - G}{G - G_{\min}} \quad (2)$$

where G , G_{\max} , and G_{\min} are, respectively, the conductance at any voltage, the maximum conductance (all channels open), and the minimum conductance (all channels closed). After substitution of Eq. 2 into Eq. 1 and taking the log transform, this linearized equation was used to process the data and obtain n and V_0 :

$$\ln \left(\frac{G_{\max} - G}{G - G_{\min}} \right) = \frac{nF}{RT} V - \frac{nFV_0}{RT} \quad (3)$$

A typical fit to the linearized data is shown in Fig. 1. The measured values of V_0 were corrected for electrode asymmetry and the liquid junction potentials at the tip of the KCl salt bridges, by subtracting the value of the reversal potential measured after the membrane had broken, after correcting this value for the calculated liquid junction across the hole, using the Nernst-Planck flux equation.

Determining the conductance/voltage relationship in the presence of a salt gradient for channels whose closed state is not only conductive but of opposite ion selectivity requires some care. A sample record is shown in Fig. 2. Proceeding from left to right (following experimental time), the voltage increased to +56 mV and then declined. As the voltage neared zero, channels began opening, as evidenced by a deviation from linearity (this is very evident with one or a few channels in the membrane). By about -20 mV, just about all of the channels were open and a linear relationship was once again obtained. At about -40 mV, the channels began to close. After the voltage reached its lowest value (-64 mV) and began to rise, channels reopened. They stayed open for a while until the voltage neared zero, when they began to close. As the voltage became more positive, all of the channels entered a closed state, resulting in a linear dependence of current with voltage. Thus lines A and D indicate the current/voltage relationship for the closed channels. Lines B and C indicate the current/

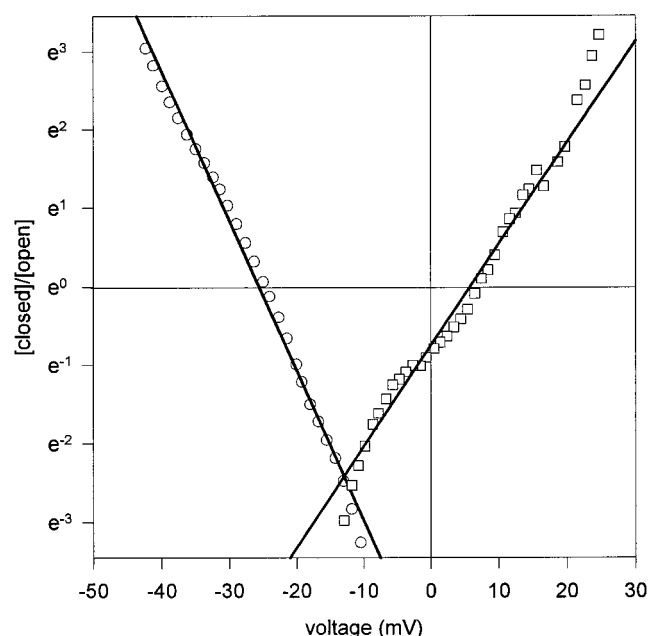


FIGURE 1 Typical fits of data to the Boltzmann distribution. These data were collected in the presence of a KCl gradient.

voltage relationship for the open channels. Because the rates of channel closure are much slower than those for channel opening (Colombini, 1979), only transitions from line A to line B and line D to line C were analyzed. Lines A and D served as the baselines for the analyses, and the intersections between lines A and B and lines C and D served as origins for the chord conductances. The reversal potentials of the open channels are estimated from the intercepts of lines B and C with the thin horizontal line that designates zero current. The reversal potentials were best estimated from single-channel or few-channel membranes. In some experiments, the presence of large numbers of channels made it difficult to determine the

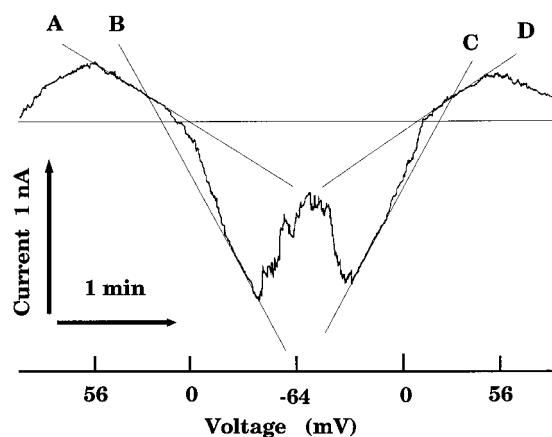


FIGURE 2 Current/voltage relationship of a multichannel membrane in the presence of a salt gradient. The *cis* compartment contained a LiCl activity of 0.60, whereas in the *trans* compartment the activity was 0.060. Both compartments also contained 1.0 mM CaCl_2 , 1.0 mM MES, pH 5.8. The indicated voltage refers to the *cis* (high salt) side. This voltage was corrected for electrode asymmetry (see Materials and Methods). The voltage was applied in the form of slow triangular waves (5.0 mHz, ± 60 mV). Time proceeded in the direction indicated by the time arrow. The thin horizontal line is the zero-current line. The lines labeled A–D are discussed in Materials and Methods.

correct slope for lines corresponding to B and C. In such cases, lines were drawn tangent to the data in the appropriate region and intersecting the zero-current line at a previously determined reversal potential.

Solutions

For each salt considered, molal activity coefficients (Robinson and Stokes, 1965) were used to make solutions of 0.60 and 0.060 activity. These were used as our standard activity gradient for all of the experiments (except for the urea experiments). Both solutions also contained 1.0 mM 2-(*N*-morpholino)ethanesulfonic acid (MES) to buffer at pH 5.8, and 1.0 mM CaCl_2 . For the urea gradient, concentrations of 1.2 and 0.12 M were used in the presence of symmetrical 1.0 M KCl, 1.0 mM MES (pH 5.8), and 1.0 mM CaCl_2 .

VDAC stocks

Mitochondrial membranes were isolated from a wall-less mutant of *Neurospora crassa* as previously described (Mannella, 1982). These were stored in dilute salt buffered at pH 7 and containing 15% (v/v) dimethyl sulfoxide. An aliquot was supplemented with Triton X-100 to a final concentration of 1.0% (v/v) before use. Aliquots of 1–5 μl were stirred into the *cis* side of the experimental chamber, and channels inserted spontaneously.

THEORY

Estimation of drift kinetic energy due to solutes

A gradient of solute necessitates an opposite gradient for water. If ideal behavior applied, these gradients would cancel out. However, the degree of coupling of the movement of solutes (especially ions) to the wall of the channel is unlikely to be identical to that of the movement of water. Thus most experiments were performed in the presence of almost identical water gradients, and thus this common effect was neglected. Clearly, all observed effects include water flow, but observed changes with different solutes reflect differences in the properties of the solutes.

To calculate the kinetic energy of an ion drifting at its terminal velocity through the VDAC channel, we started with

$$E_{\text{kin}} = \frac{mv^2}{2} \quad (4)$$

where v is the velocity. As VDAC is a large pore, the permeant species are hydrated ions, so m is the hydrated mass. The hydration numbers, taken from Robinson and Stokes (1965, p. 62), are those estimated from diffusion measurements, as these should be the most relevant to current considerations.

Velocity is the product of mobility and the driving force:

$$v = u * \text{Force} \quad (5)$$

and mobility is given by

$$u = \frac{N\lambda_0}{|z|F^2} \quad (6)$$

where N is Avogadro's number, λ_0 is the limiting equivalent conductivity for a single ion species (Robinson and Stokes, 1965), and z is the charge.

Therefore, Eq. 4 becomes

$$E_{\text{kin}} = 0.5mu^2\text{Force}^2 \quad (7)$$

Because anions and cations are subjected to different forces, they must be considered separately, and their effects combined to yield an estimate of the kinetic energy that could be contributed by the salt:

$$E_{\text{kin}} = 0.5(t_+(m_+u_+^2\text{Force}_+^2) + t_-(m_-u_-^2\text{Force}_-^2)) \quad (8)$$

where the transference numbers, t_+ and t_- , are

$$t_+ = \frac{p_+}{p_+ + p_-} = 0.5\left(1 + \frac{E}{58 \log(a_2/a_1)}\right) \quad (9)$$

$$t_- = \frac{p_-}{p_+ + p_-} = 0.5\left(1 - \frac{E}{58 \log(a_2/a_1)}\right) \quad (10)$$

These come from the Nernst/Planck equation, and the p 's are the effective ion permeabilities within the channel (see also Bockris and Reddy, 1973, p. 419). E is the reversal potential. By using these transference numbers, we are compensating for the selectivity of the channel.

Phenomenologically, the driving force consists of two components, the activity gradient and the voltage:

$$\text{Force} = \frac{1}{a}RT\frac{da}{dx} + zF\frac{dV}{dx} \quad (11)$$

where da/dx can be taken as the difference in the salt activity across the membrane (Δa), divided by an estimated thickness, x (we used 5×10^{-7} cm). Therefore Eq. 8 becomes

$$E_{\text{kin}} = 0.5t_+m_+\left(u_+\left(\frac{RT}{ax}\Delta a + V\frac{F}{x}\right)\right)^2 + 0.5t_-m_-\left(u_-\left(\frac{RT}{ax}\Delta a - V\frac{F}{x}\right)\right)^2 \quad (12)$$

Comparison with experimental observations

The shifts in the voltage-dependent behavior of VDAC channels in the presence of an ion gradient was observed as shifts in V_0 , the voltage needed to close half the channels. If the flow of ions is contributing to the energy difference between the open and closed states, this should appear as a new term in the numerator of the exponent in Eq. 1 as follows:

$$nFV - nFV'_0 - kE_{\text{kin}}(V) \quad (13)$$

k is the factor that describes the coupling between the ion flow and the gating system in VDAC. At the voltage at which half the channels are open ($V = V_0$),

$$nFV_0 = nFV'_0 + kE_{\text{kin}}(V_0) \quad (14)$$

where nFV'_0 is the value of the energy difference between the states in the absence of an ion gradient. The value

measured in symmetrical 1.0 M KCl was used. By subtracting this value, we can get at a value for the portion of the drift kinetic energy at V_0 that is coupled to VDAC's gating mechanism. Note that the n value calculated with Eq. 3 contains information relating to the voltage dependence of the kinetic energy and thus is not the value for n in Eq. 14. This value must reflect only the voltage dependence of the VDAC channel, and thus the value measured in the absence of a salt gradient was used. Therefore, the value of nFV_0 on the left side of Eq. 14 consists of the n value in symmetrical 1.0 M KCl, and the V_0 value measured in the presence of the particular salt gradient.

There is some drift kinetic energy in symmetrical KCl due to the electric field, but this effect should not lead to any asymmetry. Because of the channel's preference for anions, the drift kinetic energy should always favor the open state, i.e., interfere with channel closure. Calculations show that because of the lack of a salt gradient and the fact that the anions and cations act in opposite directions, the calculated drift kinetic energy in symmetrical salt is small. However, the calculated drift kinetic energy in the presence of a gradient was corrected by the value in symmetrical KCl, for the numbers to be comparable to the shifts in nFV_0 (these were corrected for the value in symmetrical 1.0 M KCl (Eq. 14)). This was a small correction.

When we compared the drift kinetic energy for gradients of different ions, it was necessary to account in some way for the fact that the single-channel conductances varied. This was done by multiplying the result by the single-channel conductance in nS. This was also done for the calculation of the kinetic energy for symmetrical 1.0 M KCl (4 nS).

Acetate and butyrate are partially protonated and form complexes with the cations. The amounts in each form were calculated (see Table 1) from published stability constants (Smith and Martell, 1976), and all species were considered separately. These had significant but small effects on the final results.

RESULTS

The G-V curve for VDAC is shifted laterally in the presence of an ion gradient

When reconstituted into planar membranes made of soybean phospholipids, VDAC displays two gating processes: one at positive values and the second at negative values of the potential. This causes the conductance/voltage curve to

be bell-shaped around 0 mV (Fig. 3). The gating processes are symmetrical, the gating valence (n) being very similar for both, and the midpoint potential being the same but of opposite sign. This is generally true when reconstituted into membranes consisting of soybean phospholipids, regardless of the salt species. In pure lipids, pronounced asymmetries are common, indicating the fundamental asymmetry of individual VDAC channels.

In the presence of a salt gradient, the conductance/voltage curve is no longer centered around 0 mV, but is shifted in a direction favoring the closed state for one gating mechanism and the open state for the other (Fig. 4). Thus, in the presence of an ion gradient, the work performed by (or on) the channel during the gating is increased or decreased, depending on which of the two gating processes is considered.

Simply lowering the salt concentration by 10-fold on both sides of the membrane produces no pronounced effect (Fig. 3). Thus it is the presence of the salt gradient that is causing the pronounced shifts in the voltage needed to close the channels. If the direction of the gradient is inverted, the shift is also inverted (Fig. 5), indicating that the source of the asymmetry is not the equipment or the manner in which the membrane is generated.

The shift is also observed in the presence of neutral lipids (diphytanoyl PC). Thus surface charge effects are not the fundamental cause of the phenomenon.

The shifts vary, depending on the nature of the salt used. Table 2 summarizes results obtained using various solutes. Note that, in all cases, a smaller negative potential and a

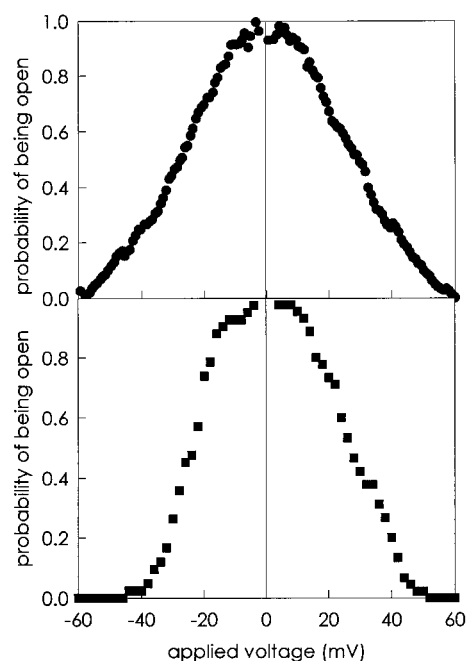


FIGURE 3 The voltage dependence of the conductance of VDAC at low and high salt. In *A*, the aqueous phases were 1.0 M KCl, 1.0 mM CaCl_2 , 5.0 mM MES (pH 5.8). This experiment was courtesy of Xiaofeng Xu. In *B*, the solutions were 0.10 M KCl, 1.0 mM CaCl_2 , 5.0 mM MES (pH 5.8).

TABLE 1 Estimated activities of different species in the acetate and butyrate experiments

Salt	Side	A^-	K^+ complex	HA
K acetate	<i>Cis</i>	0.506	0.095	0.024
	<i>Trans</i>	0.0589	0.001	0.003
Na butyrate	<i>Cis</i>	0.566	0.000	0.034
	<i>Trans</i>	0.056	0.000	0.004

Calculated using binding constants from Smith and Martell (1976).

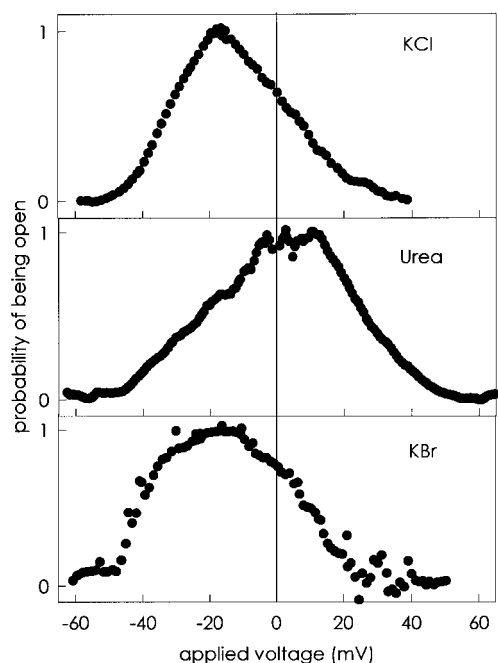


FIGURE 4 *Neurospora crassa* VDAC open probability as a function of the voltage. Conditions were 0.60 versus 0.060 activity of KCl (top), 0.60 versus 0.060 activity of KBr (bottom), and 1.2 M versus 0.12 M urea in the presence of symmetrical 1.0 M KCl (middle), across the membrane. Both solutions also contained 1.0 mM CaCl_2 , 1.0 mM MES (pH 5.8). The data were obtained from records such as that shown in Fig. 2. Only the parts of the current record where the channels were opening were analyzed, and thus the data in the figure are a combination of results from two adjacent records. See Materials and Methods for details.

larger positive potential are needed to close half the channels. The sign of the shift is consistent with the ion flow influencing the gating process.

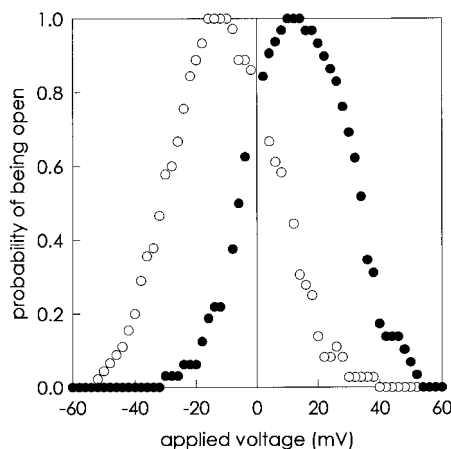


FIGURE 5 Reversing the direction of the salt gradient results in a reversed shift in the gating processes. In both experiments (open and filled symbols) a salt gradient of KCl was present (0.60 versus 0.060 activity). In the experiment illustrated with the open symbols, the voltage was controlled on the high-salt side, whereas for that illustrated by the filled symbols, the voltage was controlled on the low-salt side (the opposite side was held at virtual ground by the amplifier).

TABLE 2 Voltage dependence parameters for various salts

Salt	Gating at negative voltages		Gating at positive voltages	
	V_0 (mV)	Apparent n	V_0 (mV)	Apparent n
NaCl (3)	-34 ± 1	4.8 ± 0.1	7.3 ± 0.4	3.1 ± 0.3
KCl (2)	-28 ± 4	4.9 ± 0.5	5.2 ± 0.4	3.6 ± 0.2
LiCl (3)	-27 ± 3	5.0 ± 0.2	10 ± 1	3.3 ± 0.2
KBr (2)	-39 ± 2	4.1 ± 0.1	8.1 ± 0.4	2.8 ± 0.2
K acetate (3)	-30.6 ± 0.4	3.7 ± 0.1	0.53 ± 0.03	4.4 ± 0.5
RbBr (2)	-41 ± 2	3.4 ± 0.1	4.7 ± 0.6	2.8 ± 0.2
Na butyrate (2)	-26.5 ± 0.8	3.1 ± 0.4	12.7 ± 0.1	3.3 ± 0.2
Urea (3)	-24 ± 1	2.3 ± 0.1	25 ± 2	3.2 ± 0.2

In all cases (except for urea), the salt activity was 0.6 on the *cis* side and 0.06 on the *trans* side. The sign of the potential refers to the high-salt side, the *cis* side (*trans* is ground). The values are means \pm SE. The values in parentheses are the number of experiments performed.

The differences induced by the ion gradients in the free energy of VDAC gating correlate with the kinetic energy of the ionic drift

A great deal of evidence indicates that the voltage sensor of VDAC is located on the inner wall of the channel in the open state and translocates out of the channel during the gating process (Colombini, 1994). The voltage sensor has a net positive charge and is driven by the electric field to one membrane surface or the other, depending on the sign of the applied potential. Thus the application of a positive potential on the high-salt side would drive the sensor down the salt gradient toward the low-salt side. In contrast, the application of a negative potential would drive the sensor against the salt gradient. These considerations raise the possibility that kinetic energy from the flow of ions through the channel might be transferred to the sensor, thus changing the relative energy level of the open state compared to the closed state.

If there is a coupling between the ion flow and the movement of the sensor, there should be a correlation between the shift in the energy of the gating process and the kinetic energy of the salt flowing through the channel. The

TABLE 3 Partitioning the conductance between cation and anion

Salt	Reversal potential (mV)	Single-channel conductance (nS)	Transference number of cation	Partitioned conductance (nS)	
				Cation	Anion
NaCl (6)	14.1 ± 0.9	1.88 ± 0.06	0.38	0.71	1.17
KCl (2)	14.0 ± 0.8	1.71 ± 0.01	0.38	0.65	1.06
LiCl (5)	20.9 ± 0.7	1.30 ± 0.03	0.32	0.42	0.88
KBr (8)	11.3 ± 0.4	1.80 ± 0.05	0.40	0.72	1.08
RbBr (3)	10.0 ± 0.0	1.90 ± 0.04	0.41	0.79	1.11
K acetate (5)	6.5 ± 0.2	0.78 ± 0.01	0.44	0.35	0.43
Na butyrate (2)	4.8 ± 0.2	0.84 ± 0.01	0.46	0.39	0.45

The salt gradient was 0.60 activity (*cis*) versus 0.060 activity (*trans*), with 1.0 mM CaCl_2 and 1.0 mM MES (pH 5.8) added to both. The side defined as *trans* was kept at ground potential. VDAC from *Neurospora crassa* was used. Data are mean \pm SEM. The number of experiments is in parentheses.

TABLE 4 Properties of ions used in the experiments

Ion	Mass (g/mol)	Hydration (no. of waters)	Total mass (g/mol)	Mobility $\times 10^9$ ($\text{cm}^2 \text{mol}^{-1} \text{s}^{-1}$)
Li^+	6.9	5.7	109.6	4.15
Na^+	23.0	2.9	75.3	5.38
K^+	39.1	0.2	42.7	7.89
Rb^+	85.5	0	85.5	8.36
Cl^-	35.5	0.5	44.5	8.20
Br^-	79.9	0	79.9	8.39
Acetate	59.0	0	59.0	4.39
Butyrate	87.1	0	87.1	3.50

The hydration numbers are from Robinson and Stokes (1965, p. 62). The ionic mobilities were calculated according to Eq. 6, with the limiting equivalent conductivities from Robinson and Stokes (1965).

effective drift kinetic energy is proportional to the mass times the drift velocity squared (see Materials and Methods). Thus this hypothesis was tested by using salts composed of ions of different mobilities and masses (Table 4).

To estimate the kinetic energy according to Eq. 12, it was necessary to estimate the transference numbers from the reversal potentials (Table 3). This varied, as expected, with the salt used, but more importantly, the amount of conductance attributed to each ion depended strongly on the nature of the counterion. An ion's permeability declines if it is paired with a less permeable or less mobile counterion. This is a consequence of the large size of the pore and the interaction among the multiple ions likely to be present within the pore at any time.

The calculated drift kinetic energy (Table 5) is plotted versus the observed change in the free energy difference between the open and closed states (Fig. 6). The difference in the magnitude of the energies is at least partly explained by the fact that the kinetic energy refers to one ion, and the ion flow through the channel is $\sim 10^8$ ions/s. The inorganic

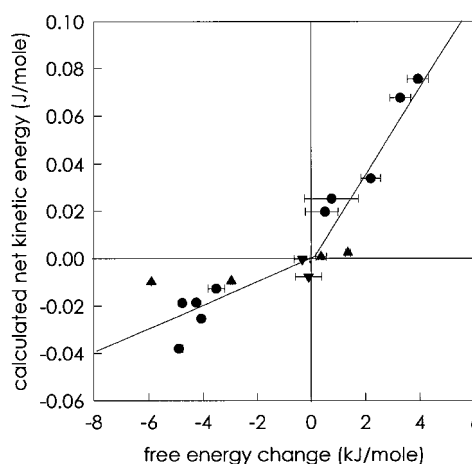


FIGURE 6 Correlation between the drift kinetic energy per ion flowing through the channel, with the shift in the channel-gating energetics measured in the presence of a 10-fold activity gradient. The values are from Table 5: ●, inorganic salts; ▲, salts of butyrate and acetate; ▼, urea.

salts (plotted as circles) form a reasonable straight line. The salts of acetate and butyrate (triangles) seem to have a proportionately stronger effect on VDAC.

The effects of the ion gradient are not attributable to a water activity gradient, reversal potential, or differences in hydrostatic pressure or ion mobilities

Urea was used as a control for the osmotic pressure difference that exists when an ion gradient is present. Osmotic gradients have been shown to give rise to streaming potentials in narrow channels due to a coupling of water flow to ion flow (Rosenberg and Finkelstein, 1978). For the highly

TABLE 5 Calculations of net kinetic energy

Salt	V_0 (mV)	E_{kin} cation (J)	E_{kin} anion (J)	$E_{\text{kin}} \times G$ total (J)	E_{kin}^* tot. corr. (J)	Change in nFV_0 (kJ)
LiCl	10.4	-0.0030	-0.0036	-0.009	-0.013	-3.52 ± 0.31
NaCl	7.35	-0.0036	-0.0040	-0.015	-0.019	-4.26 ± 0.10
KCl	5.2	-0.0041	-0.0045	-0.015	-0.019	$-4.78^{+0.10}_{-0.07}$
KBr	8.1	-0.0049	-0.0069	-0.021	-0.025	-4.08 ± 0.10
RbBr	4.7	-0.0097	-0.0082	-0.034	-0.038	$-4.90^{+0.14}_{-0.12}$
K acetate	0.53	-0.0036	-0.0018	-0.006	-0.010	-5.90 ± 0.01
Na butyrate	12.7	-0.0054	-0.0009	-0.006	-0.010	$-2.97^{+0.05}_{-0.02}$
Urea	24.6			-0.004	-0.004	-0.10 ± 0.48
LiCl	-27.1	0.0002	0.0178	0.023	0.020	$0.51^{+0.48}_{-0.72}$
NaCl	-34.1	0.0001	0.0197	0.037	0.034	2.20 ± 0.36
KCl	-28.1	0.0003	0.0167	0.029	0.025	0.75 ± 0.99
KBr	-38.6	0.0000	0.0398	0.072	0.068	3.28 ± 0.39
RbBr	-41.3	0.0000	0.0419	0.080	0.076	3.93 ± 0.39
K acetate	-30.6	0.0002	0.0059	0.006	0.002	1.35 ± 0.10
Na butyrate	-26.5	0.0004	0.0050	0.005	0.001	0.36 ± 0.19
Urea	-23.6			0.004	0.004	-0.34 ± 0.29

*After we summed the drift kinetic energy for the ions and multiplied by G (the single-channel conductance in nS), the calculated drift kinetic energy for symmetrical 1.0 M KCl at ± 25 mV was subtracted to reflect the fact that this is contributing to the control value of nFV_0 . This control value of nFV_0 (6.03 kJ/mol) was subtracted from the measured nFV_0 value for each of the salts to obtain the listed change in nFV_0 . In the case of acetate and butyrate, in addition to the values shown for the individual ions, the total drift kinetic energy includes small contributions from acetic acid, butyric acid, and K acetate complex.

cation-selective gramicidin channel, a 2 M urea gradient produced a 2.5-mV streaming potential. With the lower selectivity and large pore size of VDAC, such effects should be trivial. Indeed, as seen by the inverted triangles, 1.2 M urea versus 0.12 M urea had no significant effect on the energetics of the channels (Figs. 4 and 6). Being insensitive to the electrical component of the driving force, it has a small calculated drift kinetic energy. Possible confounding effects of urea on the activity of the otherwise symmetrical KCl solution were dismissed, based on the observations of Rosenberg and Finkelstein (1978).

No correlation could be found between the shift in the energetics of VDAC gating and the salt mobilities or the channel reversal potential for these salts (Fig. 7, *A* and *B*). This indicates that differences in mobilities alone, and therefore terminal velocity, cannot account for our results. The hydrated masses of the permeant species have to be taken into account.

There is a correlation between the difference in the densities of the solutions and the energy changes in VDAC (Fig. 8). Thus the possibility that this density difference could result in the flow of solution through the membrane and thus produce the observed results on VDAC was tested by applying a hydrostatic pressure difference across the membrane. The experiments were done in the presence of symmetrical 1.0 M KCl, but the level of the solution on one side of the membrane was higher than the other. A 0.5–2-mm difference in water pressure caused no reproducible energy shifts in VDAC, as measured in the presence of symmetrical 1.0 M KCl solution. These transmembrane hydrostatic pressures are far higher than the maximum 10% difference in density between the salt solutions in the pres-

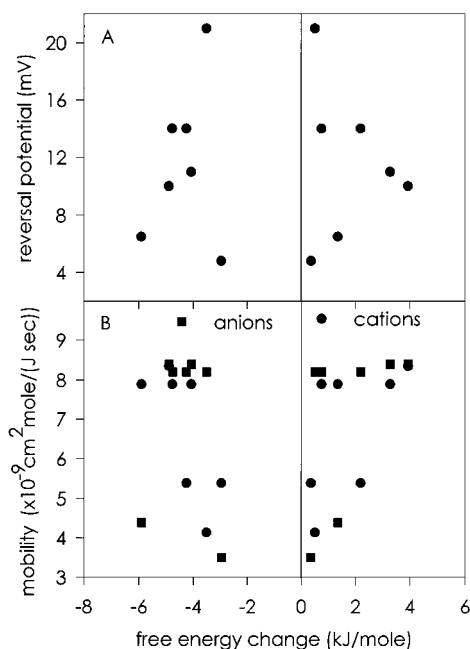


FIGURE 7 Lack of correlation between the ion mobilities or the measured reversal potentials with the shift in the energetics of gating.

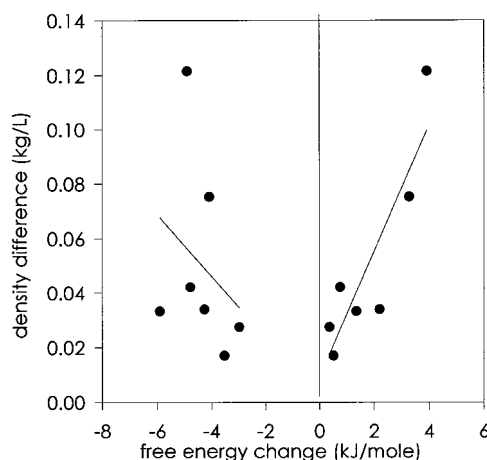


FIGURE 8 Correlation between difference in density between the salt solutions on either side of the membrane and the shift in the voltage-gating energetics of VDAC. The correlation coefficients are 0.89 and 0.3, respectively, for data for positive and negative free energy change. The former is significant at the 99% confidence level; the latter is not significant.

ence of an ion gradient and a total water level above the membrane between 0.1 and 0.5 mm (the levels were about equal).

DISCUSSION

The large pores formed by VDAC channels may be able to hold as many as 1000 water molecules. Hence it should not be surprising that flow through these channels begins to resemble bulk flow. Just as the flow of fluid through pipes transfers energy to the wall of the pipe because of friction, the net flow of substances through the aqueous pore of VDAC should transfer energy to the walls of the pore. In the case of VDAC, there is strong evidence (Peng et al., 1992; Thomas et al., 1993) that the domain of the protein whose movement is responsible for voltage gating forms part of the wall of the pore. Of the 12 β -strands and one α -helix believed to form the wall of the pore, there is evidence (Peng et al., 1992; Thomas et al., 1993) that the α -helix and six of the β -strands are involved in this motion. This motion has a major component normal to the plane of the membrane. Therefore, collisions of moving ions within the pore should be able to bias the motion.

The presence of a gradient of free energy in an aqueous solution of ions results in a biasing of the otherwise random motion of the ions. This biased motion results in a drift of the ions down their gradient in free energy. This drift has an associated drift kinetic energy (derived in the Theory section) that is transferred to the wall of the channel or to the bulk phase as heat. We do not know what fraction of the energy is imparted to the wall of the pore, but the total drift kinetic energy is potentially very large. For example, in the case of the KCl gradient, -28 mV on the high-salt side is needed to close half the channels. Under these conditions, the calculated drift kinetic energy for Cl^- was 0.017 J/mol

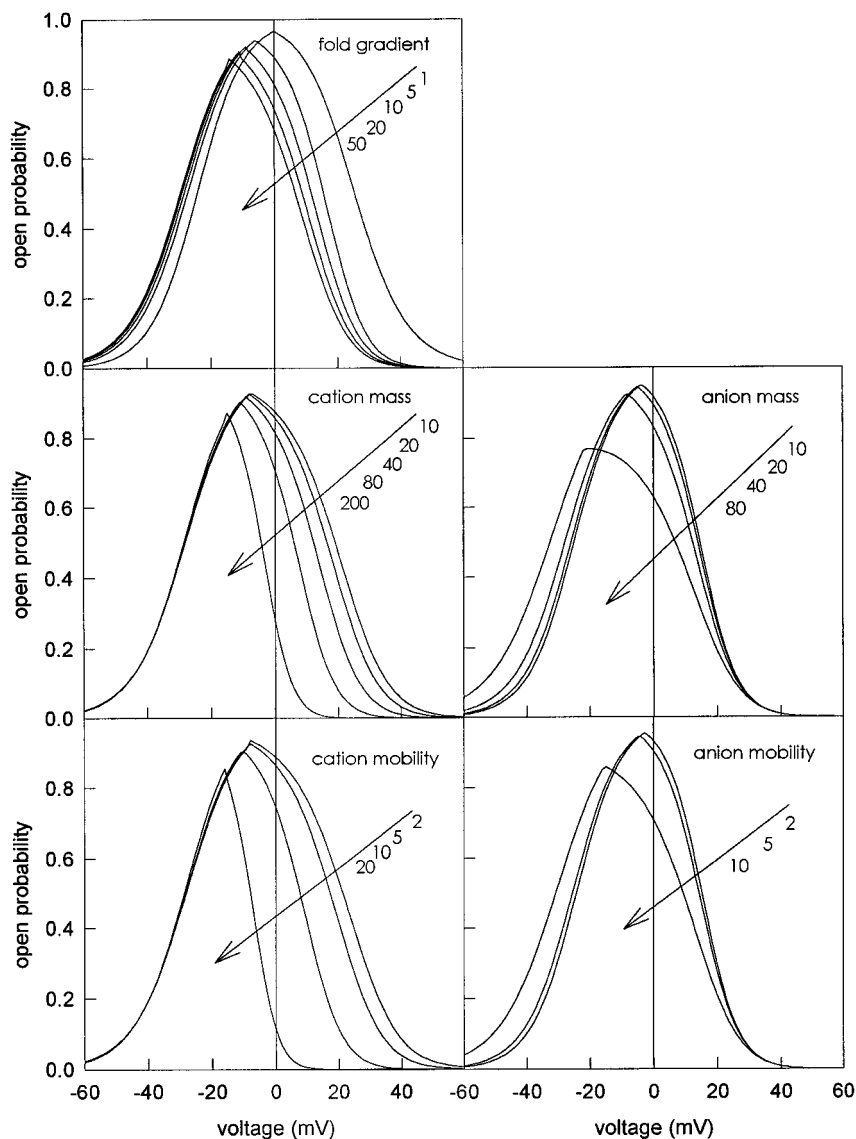
(that for K^+ is negligible under these conditions). Clearly, the collision of a single Cl^- ion would not be sufficient to favor the open state by 750 J/mol. However, the combined effect of the flow, under these conditions of $\sim 4 \times 10^8$ ions/s would result in a total drift kinetic energy of ~ 7000 kJ/s · mol.

Whether this is enough energy to account for the observed shift in the energetics of the channel depends on how this cooperative effect could come about. The residency time of an ion in VDAC is much shorter than the estimated time for the channel to undergo a conformational change ($\sim 1 \mu s$). Thus, as ions flow through the pore, their collisions with amino acid side chains extending into the pore could result in a sustained mechanical stress that would either favor or disfavor channel closure. In the current model, the hydrogen bonding that links the β -strands that form the mobile sensor to those in the rest of the β -barrel would need to be broken for gating to occur. The stress induced by the ion flow could be manifested as a distortion in these hydrogen bonds, thus favoring the motion. The

opposite flow could make it more difficult for the electric field to cause enough distortion of these bonds and thus produce closure. It is interesting that in Fig. 6, the drift kinetic energy seemed to be more effective (shallower slope) at destabilizing the hydrogen bonds and inducing closure (negative free energy change) than at stabilizing the open state (positive free energy change).

It is worth considering the possibility that the aqueous medium plays a role in transferring energy to the walls of the pore. In aqueous solution (as opposed to vacuum), ions accelerate only very briefly when a force is applied, reaching a terminal velocity because of friction with the medium. The calculations of net kinetic energy do not take into account the fact that energy, continuously imparted to the medium because of friction, will cause the medium to have a net motion in the direction of ion flow. The motion of the medium can also be transferred to the walls of the pore. This energy transfer would be in addition to that considered in the previous paragraph.

FIGURE 9 Theoretical calculations of the shifts in the voltage dependence of the open probability caused by varying factors in the theoretical equation. The general conditions are a KCl gradient with activities at 0.6 and 0.06, and the potential refers to that on the high-salt side. When the gradient was varied, the activity on the high-salt side was increased. When the ion masses (in atomic mass units) or mobilities ($\times 10^9 \text{ cm}^2 \text{ mol}^{-1} \text{ s}^{-1}$) were varied, the values for the counter-ion were those of either K^+ or Cl^- , as appropriate. The factor k in Eq. 13 was taken as 50,000 for negative potentials and 290,000 for positive potentials. (Values derived from Fig. 6.)



Because there is a gradient of water, there should be a tendency for water to flow in the direction opposite that of solute flow. By using a urea gradient, we showed that such a flow has no significant effect on the gating process. This could be explained by a difference in the effective coupling between water and ions and the walls of the channel. Indeed, there is evidence that the aqueous content of the channel is not uniform, but that a shell of water next to the channel wall may behave differently from the water in the center of the pore (Zambrowicz and Colombini, 1993).

The hypothesis that ion flow through the channel imparts energy to the voltage sensor of VDAC, and thus biases the voltage-gating process, was tested by using ions of varying mobility and mass. A reasonable correlation was obtained between the calculated drift kinetic energy of the ions in the channel and the shift in free energy difference between the open and closed states. No correlation was observed with other properties of the ions, except for the density of the solution. The possibility that pressure differences across the channel, due to differences in the density of the solutions on either side of the membrane, could be responsible for the observed changes in channel properties, was tested by applying hydrostatic pressure differences across the membrane. These had no reproducible effect. Under the conditions studied, the drift kinetic energy per water molecule would be less than 10^{-17} J/mol. Even considering that the water concentration is two orders of magnitude higher than the salt concentration, the kinetic energy is far too low, because the pressure differences were very small (less than 10^{-4} atm). Therefore, the only plausible cause for the shift in the energetics of the channel is the kinetic energy imparted by the ionic flow.

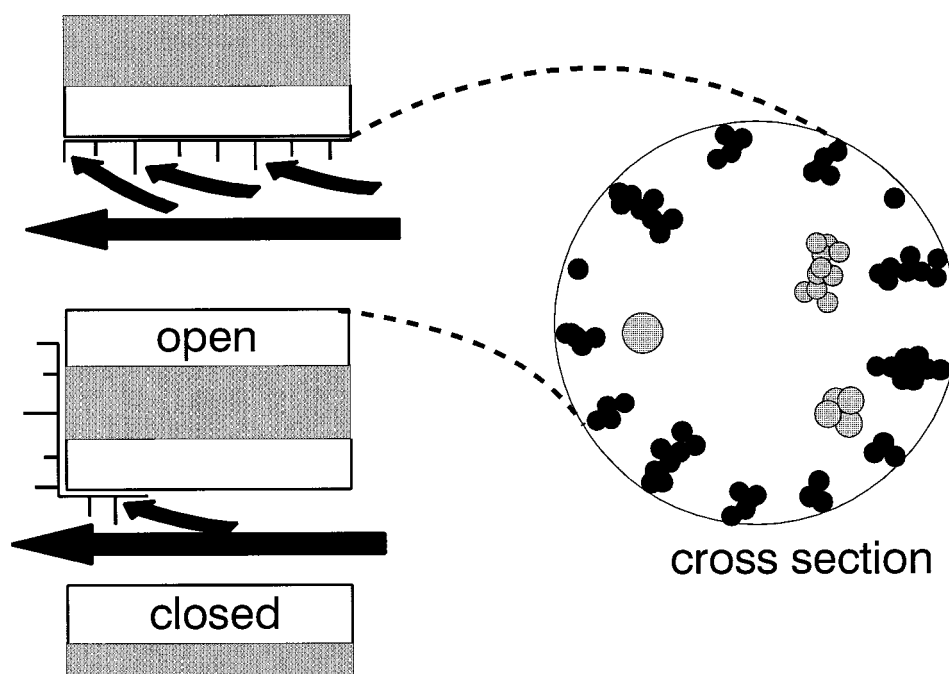
The magnitude of this kinetic energy is influenced by a number of factors, including the magnitude of the ion gra-

dient and the mass and mobility of the ions. Using estimated degrees of coupling from Fig. 6, one can obtain theoretically expected shifts in the voltage dependence of the open probability as a result of changing the drift kinetic energy in various ways (Fig. 9). Although the direction of the change is predictable, the magnitude of the change and the shape of the curves hint at the underlying complexity.

Experimentally, the situation is even more complex, because the open probability is influenced by factors not included in the theory. The scatter in the data in Fig. 6 could arise from different degrees of coupling between ions and the protein's mobile domain, depending on the chemical nature of the ion. The especially large divergences seen with acetate and butyrate might arise from increased friction with the walls of the pore. After all, butyrate and acetate are the only ions with apolar regions. Perhaps these associate transiently with apolar regions in the amino acid side chains that extend into the channel (Fig. 10). Another factor may be that impermeants favor channel closure by inducing a hydrostatic pressure difference between the inside of the pore and the bulk solution. This has been shown clearly by the use of dextran and polyethylene glycol (Zimmerberg and Parsegian, 1986). Partial effects could be induced by the larger ions. In the closed state, the very low permeability of anions may induce some hydrostatic pressure differences. Perhaps these explain why butyrate and acetate have a much stronger effect on closing the channels than expected from the kinetic energy calculations (*left side* of Fig. 6).

The direction of the energetic shift resulting from the ion gradient is consistent with the working model for VDAC gating (Fig. 11). The mobile, voltage-sensing domain is a positively charged region (*black region in the figure*). VDAC undergoes closure at both positive and negative potentials as a result of the movement of this domain down

FIGURE 10 A schematic view of sections through the VDAC channel, illustrating how kinetic energy could be transferred between the flowing ions and the mobile sensor domain. A cross section through VDAC's pore shows side chains (black) of the amino acids lining the pore extending into the lumen, where they contribute to the selectivity of the channel. The translocating ions (gray) could collide with these side chains and transfer some kinetic energy. In longitudinal section, the ion flow (black arrows) is shown colliding, in part, with the extended side chains driving the β strand (the sensor) out of the channel, resulting in the closed state.



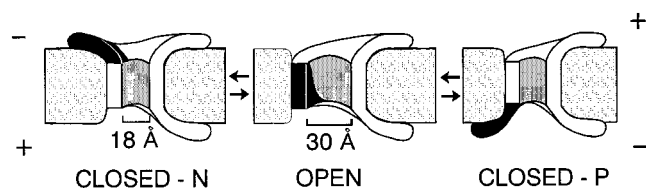


FIGURE 11 The voltage gating mechanism for VDAC from the literature (Colombini et al., 1996). The black region represents the voltage sensor, the domain that moves in response to changes in transmembrane potential. A positive potential on top drives the domain downward, and vice versa. There are two different closed states: one closed at negative potentials (closed-N), and the other at positive potentials (closed-P). The dimensions indicated are the estimated pore diameters in the open and closed states.

the electrical gradient. The closed state achieved with positive potentials is therefore fundamentally different from that achieved with negative potentials. In the presence of a salt gradient, application of a positive potential to the high salt side would drive the sensor toward the low-salt side, inducing closure. The salt gradient would favor this motion. Thus lower positive potentials should be needed to close the channel. The application of a negative potential would draw the sensor toward the high-salt side. In this case, the ion flow would interfere with the motion and favor the open state. Thus higher voltages should be needed to close the channels. These expectations are exactly what was observed, and therefore the observations are in harmony with the gating mechanism developed to account for other experimental results (Colombini, 1994).

It is difficult to know how general these observations are and whether they have any physiological significance. The list of membrane channels that form large pores is growing (e.g., connexins, fusion pores, protein translocation pores, some toxins like colicins, complement attack complex, and bacterial porins). Only appropriate experiments could test whether similar phenomena occur in these channels. There are physiological conditions in which large ion gradients exist across channels, yet to date we know of no report that attributes any effect of ion flow (not simply ion binding or blockage) to the probability of finding the channel in a particular conformation. Clearly, it is crucial that the movement of the voltage sensor be somehow coupled to the ion flow, and in some channels the sensor is believed to be distal from the site of ion permeation. Whether this is a physiologically relevant or general phenomenon or not, the observation of the coupling of ion flow to gating of VDAC gives important insight into and confirmation of the gating process in this channel.

This work was supported by ONR grant N00014-90-J-1024, by National Institutes of Health Grant GM 35759, and JSM-RT Grant 69602 to MZ. MZ is supported by the Belgian Ministry of Defence.

REFERENCES

- Bockris, J. O'M., and A. K. N. Reddy. 1973. *Modern Electrochemistry*. Plenum Press, New York.
- Catterall, W. A. 1986. Voltage-dependent gating of sodium channels: correlating structure and function. *Trends Neurosci.* 9:7–10.
- Colombini, M. 1979. A candidate for the permeability pathway of the outer mitochondrial membrane. *Nature*. 279:643–645.
- Colombini, M. 1987. Characterization of channels isolated from plant mitochondria. *Methods Enzymol.* 148:465–475.
- Colombini, M. 1994. Anion channels in the mitochondrial outer membrane. *Curr. Top. Membr.* 42:73–101.
- Colombini, M., E. Blachly-Dyson, and M. Forte. 1996. VDAC, a channel in the outer mitochondrial membrane. In *Ion Channels*, Vol. 4. T. Narahashi, editor. Plenum Publishing, New York.
- Ehrenstein, G., H. Lecar, and R. Nossal. 1970. The nature of the negative resistance in bimolecular lipid membranes containing excitability-inducing material. *J. Gen. Physiol.* 55:119–133.
- Mannella, C. 1982. Structure of the outer mitochondrial membrane: ordered arrays of pore-like subunits in outer-membrane fractions from *Neurospora crassa* mitochondria. *J. Cell Biol.* 94:680–687.
- Merrill, A. R., and W. A. Cramer. 1990. Identification of a voltage-responsive segment of the potential-gated colicin E1 ion channel. *Biochemistry*. 29:8529–8534.
- Montal, M., and P. Mueller. 1972. Formation of bimolecular membranes from lipid monolayers and a study of their electrical properties. *Proc. Natl. Acad. Sci. USA*. 69:3561–3566.
- Peng, S., E. Blachly-Dyson, M. Forte, and M. Colombini. 1992. Large scale rearrangement of protein domains is associated with voltage gating of the VDAC channel. *Biophys. J.* 62:123–135.
- Robinson, R. A., and R. H. Stokes. 1965. Appendix. In *Electrolyte Solutions*, 2nd ed. Butterworths, London. 62, 463.
- Rosenberg, P. A., and A. Finkelstein. 1978. Interaction of ions and water in gramicidin A channels. Streaming potentials across lipid bilayer membranes. *J. Gen. Physiol.* 72:327–340.
- Schein, S. J., M. Colombini, and A. Finkelstein. 1976. Reconstitution in planar lipid bilayers of a voltage-dependent anion-selective channel obtained from *Paramecium* mitochondria. *J. Membr. Biol.* 30:99–120.
- Smith, R. M., and A. E. Martell. 1976. *Critical Stability Constants*. Plenum, New York.
- Thomas, L., E. Blachly-Dyson, M. Colombini, and M. Forte. 1993. Mapping of residues forming the voltage sensor of the VDAC channel. *Proc. Natl. Acad. Sci. USA*. 90:5446–5449.
- Thomas, L., E. Kocsis, M. Colombini, E. Erbe, B. L. Trus, and A. C. Steven. 1991. Surface topography and molecular stoichiometry of the mitochondrial channel, VDAC, in crystalline arrays. *J. Struct. Biol.* 106:161–171.
- Zambrowicz, E. B., and M. Colombini. 1993. Zero-current potentials in a large membrane channel: a simple theory accounts for complex behavior. *Biophys. J.* 65:1093–1100.
- Zimmerberg, J., and V. A. Parsegian. 1986. Polymer inaccessible volume changes during opening and closing of a voltage-dependent ionic channel. *Nature*. 323:36–39.